EJTAS ISSN 2786-7447
EUROPEAN JOURNAL OF THEORETICAL AND APPLIED SCIENCES
OPEN ACCESS
PEER REVIEWED

Mathematical Analysis of Spread and Control of Diphtheria with Emphasis on Diphtheria Antitoxin Efficiency

Ngozika J. Egbune, Eloho B. Akponana, Eirene O. Arierhie, Akindele M. Okedoye
Department of Mathematics, Federal University of Petroleum Resources, Effurun, Nigeria

Suggested Citation

Egbune, N.J., Akponana, E.B., Arierhie, E.O. & Okedoye, A.M. (2024). Mathematical Analysis of Spread and Control of Diphtheria with Emphasis on Diphtheria Antitoxin Efficiency. *European Journal of Theoretical and Applied Sciences, 2*(3), 152-172.
DOI: 10.59324/ejtas.2024.2(3).14

Abstract:

Diphtheria, a bacterial infection caused by Corynebacterium diphtheriae, remains a significant public health concern worldwide. In this study, we employ mathematical modeling to analyze the spread and control of diphtheria, focusing on the efficacy of Diphtheria Antitoxin in mitigating the disease's impact. Through the development of compartmental models, system of differential equations governing the dynamics was formulated. Due to the complexity and non-linearity of the dynamics, a numerical solutions that utilizes Runge-Kutta Fehlberg order 4 and 5 method. The dynamics of diphtheria transmission and the potential impact of DAT administration on disease outcomes was investigate. Our findings highlight the critical role of Antitoxin efficiency in reducing disease burden, preventing severe cases, and containing epidemic spread. By exploring various scenarios and parameter sensitivities, we provide insights into optimal control strategies and intervention measures to combat diphtheria outbreaks effectively. This research contributes to a better understanding of diphtheria epidemiology and informs public health policies aimed at enhancing vaccination coverage and DAT availability to achieve sustainable disease control and prevention.

Keywords: *Diphtheria, AntiToxin, basic reproduction number, stability, pandemic.*

Introduction

Diphtheria is an infectious disease caused by the strains of bacteria called Corynebacterium diphtheriae that makes a toxin which causes people to get very sick (CDC, 2021). It primarily affects the respiratory system but can also affect other parts of the body. Diphtheria is a potentially life-threatening condition that can lead to severe complications if left untreated. The symptoms usually start 2–5 days after exposure to the bacteria. Typical symptoms of the infection include sore throat, fever, swollen neck glands and weakness. Within 2-3 days, the dead tissue in the respiratory tract forms a thick, grey coating that can cover tissues in the nose, tonsils and throat making it hard to breathe and swallow (NHS, 2022). The bacteria spreads from person to person, usually through respiratory droplets like from coughing or sneezing. People can also get sick from touching infected sores or ulcers. Those at increased risk of getting sick include: people in the same household, people with a history of frequent or close contact with the patient (CDC, 2022).

Treatment involves antibiotics and diphtheria antitoxin, while prevention relies on timely vaccination Lamichhane and Radhakrishnan (2022), Britannica (2023). Mathematical models aid in understanding transmission dynamics and shaping public health strategies Oli et al. (2006),

Sweileh (2022). Various authors have explored diphtheria dynamics, noting the role of contaminated environments and the necessity of booster vaccines Islam (2018), Husain (2019), Izzati et al. (2020), Kanchanarat et al. (2022), Ghani et al. 2022, Akhi et al. (2023), Amalia (2022), Rahmi & Pratama (2023), Djaafara (2020).

Statistics and findings from model calculations provided some information relevant for the spread of the disease, such as the incubation time being between 0 and 14 days and that the transmission time was found to be in an interval between 5 and 7 days. However, a method for determining what are the conditions for a mild or severe outcome of the infection has remained elusive (Famulare 2020; Ikejezie 2019). One of the criteria for measuring the spread of the disease established in the literature is the number of people infected by a previously infected person, known as the base reproduction number R. This estimates how fast the disease spreads and whether political decisions and measures are sufficient to limit its growth of the disease (Coburn et al. 2009; Delamater et al. 2019; Egger et al. 2017; Ferguson et al. 2006; Guerra et al. 2017; Kucharski et al. 2015; Lipsitch et al. 2023; Milligan and Barrett 2015; Nishiura and Chowell 2014; Thompson et al. 2019; Truelove et al. 2020; Wallinga and Teunis 2004; Wu et al. 2020). For $R > 1$ the situation turns supercritical and the total number of infected individuals rises exponentially and without control. In order to be able to predict the time evolution of the pandemic we can make use of mathematical models that were developed for other epidemics, and the following describes some of the more common models.

In the work of Amalia and Toaha (2022) diphtheria transmission dynamics in a particular region was examined, highlighting factors impacting disease spread. However, they do not delve into optimizing control strategies or incorporate multiple compartments and parameters in their model, while the mathematical model by Izzati (2020) addresses diphtheria transmission, emphasizing vaccination coverage and treatment effectiveness but neglects factors like partial immunity, progression rates, and compartment dynamics.

Notably, some models omit environmental factors and vaccine booster effects Djaafara, et al. (2020) Kanchanarat (2022). Emphasizing childhood vaccination completion and booster shots for adolescents and adults is crucial to controlling the disease, given its environmental transmission component. It is important to emphasize that the vaccine for diphtheria is among the childhood vaccinations expected to be completed by five years of age which wanes off after ten years giving room for vaccine boosters for adolescents and adults. Also, the indirect transmission of diphtheria disease via a contaminated environment contributes to the spread of the disease.

Therefore, aims to develop mathematical models analyzing factors contributing to diphtheria transmission and potential control strategies. This study is expected to enhance our scientific non-clinical understanding and policy response for tackling the persistent challenge of diphtheria prevalence. Insights from such models may guide evidence-based interventions to eliminate diphtheria worldwide.

Hence, the work of Amalia and Toaha (2022) is considered a motivation for this study, and it will be extended in the following ways;

- The vaccinated population will be split into two sub-populations, complete childhood vaccination and vaccine booster,
- The inclusion of contaminated environment population with logistic growth, temporary immunity of vaccine booster and recovery of humans,
- Inclusive of the global sensitivity analysis of the parameters on the transmission dynamics of the disease.

Modeling of the Problem

Considering the aforementioned extension conditions, divides the population into different compartments based on their disease status. This include susceptible individuals (S), exposed but

not yet infectious (H_a), latent/incubating infection (H_u), symptomatic infected (I_s), asymptomatic infected (I_a), quarantined individuals (Q), recovered with partial immunity (R_p), and recovered with full immunity (R_f). The equations govern the rate of change of individuals in each compartment over time and the transitions between compartments are influenced by various parameters, including infection rates, recovery rates, and control measures including vaccination, treatment, exposure, latency, isolation, recovery, and progression rates.

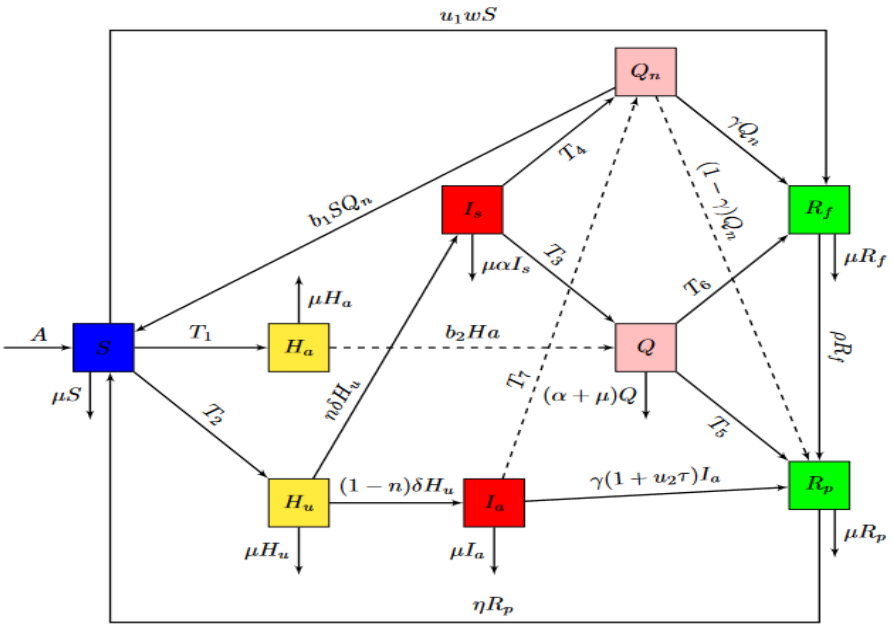

Figure 1. Compartmental Model of Diphtheria Transmission Dynamics

Using the schematic model of diphtheria transmission depicted in Fig.1, the following set of differential equations are obtained:

$$\frac{dS}{dt} = A + b_1SQ_n + \eta R_p - \mu S - T_1H_a - T_2H_u - u_1wS \quad (1)$$

$$\frac{dH_u}{dt} = T_2H_u - \mu H_u - n\delta H_u - (1-n)\delta H_u \quad (2)$$

$$\frac{dH_a}{dt} = T_1H_a - \mu H_a - b_2H_a \quad (3)$$

$$\frac{dI_s}{dt} = n\delta H_u - \mu\alpha I_s - T_3I_s - T_4I_s \quad (4)$$

$$\frac{dI_a}{dt} = (1-n)\delta H_u - T_7I_a - \mu I_a - \gamma(1+u_2\tau)I_a \quad (5)$$

$$\frac{dQ}{dt} = b_2H_a + T_3I_s - (\mu+\alpha)Q - T_5Q - T_6Q \quad (6)$$

$$\frac{dQ_n}{dt} = T_7I_a + T_4I_s - b_1SQ_n - (1-n)\gamma Q_n - \gamma nQ_n - \mu Q_n \quad (7)$$

$$\frac{dR_p}{dt} = \gamma(1+u_2\tau)I_a + T_5Q + \rho R_f + (1-\gamma)Q_n - (\eta+\mu)R_p \quad (8)$$

$$\frac{dR_f}{dt} = u_1 wS + T_6Q + \gamma Q_n - (\rho+\mu)R_f \quad (9)$$

It is assumed that the initial conditions are $S(0) > 0, H_a(0) > 0, H_u(0) > 0, I_s(0) > 0, I_a(0) > 0, Q(0) > 0, Q_n(0) > 0, R_p(0) > 0, R_f(0) > 0$ and all parameters in Table 1 (below) are positive.

These new assumptions fill the gap in the existing literature by providing a more comprehensive framework for understanding and addressing diphtheria outbreaks in developing countries. The modification made in this model is expected to provide a better result in addressing diphtheria because it incorporates a multidimensional approach and optimization strategies.

Table 1. Parameters and Their Meaning

Parameter	Meaning
Λ	recruitment rate
u_1	vaccination coverage
u_2	treatment coverage
T_1	exposure rate
T_2	latency rate
T_3	isolation rate
T_4	progression rate from symptomatically infected to not quarantined
T_5	recovery rate with treatment to partial immunity
T_6	recovery rate with treatment to full immunity
T_7	progression rate from asymptomatically infected to not quarantined
b_1	treatment success probability
b_2	progression rate from exposed to quarantined
μ	natural mortality rate
α	disease induced mortality rate
ϱ	rate of losing immunity
τ	treatment effectiveness
η	rate of regaining susceptibility
γ	recovery rate without treatment
δ	progression rate from latent to infected
w	vaccine effectiveness
$n\delta$	rate of infectiousness
$(1-n)\,\delta$	rate of asymptomatic infectiousness

Analysis of the Model

Qualitatively study the dynamical properties of the system of equations of the model (1) – (9) as examined through the following spectrum.

Bound on the Solution Space

The model assumes a closed population, where births, deaths and migration cancelled out. This assumption allows us to focus solely on the dynamics of diphtheria transmission within the population under consideration without the influence of external factors. Such that the total population is given by $N(t) = S(t) + H_u(t) + H_a(t) + I_a(t) + I_S(t) + Q(t) + Q_n(t) + R_P(t) + R_f(t)$ at any time t.

Therefore, adding all the equations of the system together, gives

$$\frac{dS}{dt} + \frac{dH_u}{dt} + \frac{dH_a}{dt} + \frac{dI_a}{dt} + \frac{dI_s}{dt} + \frac{dQ}{dt} + \frac{dQ_n}{dt} + \frac{dR_p}{dt} + \frac{dR_f}{dt} = \Lambda - \mu S - \mu H_u - \mu H_a - \mu\alpha I_s - \mu I_a - (\mu+\alpha)Q - \mu Q_n - (\mu)R_p - (\mu)R_f$$

That is

$$\frac{d}{dt}(S(t) + H_u(t) + H_a(t) + I_a(t) + I_S(t) + Q(t) + Q_n(t) + R_P(t) + R_f(t)) = \Lambda - \mu(S + H_u + H_a + I_a + I_s + Q + Q_n + R_p + R_f + \mu(1-\alpha)I_s - (\alpha)Q \quad (19)$$

Such that

$$\frac{d}{dt}(N(t)) = \Lambda - \mu N(t) + \mu(1-\alpha)I_s - (\alpha)Q \quad (11)$$

Choosing the parameters μ and α carefully such that $\mu(1-\alpha)I_s - (\alpha)Q > 0, \forall\, t$, Thus,

$$\frac{dN(t)}{dt} \geq \Lambda - \mu N(t) \tag{12}$$

Integration (11) gives

$$N(t) \geq \frac{\Lambda}{\mu} + ke^{-\mu t} \tag{13}$$

But at $t = 0$,

$$N(0) \geq \frac{\Lambda}{\mu} + k \Longrightarrow$$
$$N(t) \geq \frac{\Lambda}{\mu} + \left(N(0) - \frac{\Lambda}{\mu}\right)e^{-\Omega t} \tag{14}$$

Positivity and Boundedness

For the model to be epidemiologically meaningful and mathematically well posed, it is necessary to establish that all solutions of system with positive initial data will remain positive for all times $t > 0$. This will be established in the following theorem.

Theorem 3.1 (Positivity of Solution):

$$\frac{dS}{dt} = \frac{dH_u}{dt} = \frac{dH_a}{dt} = \frac{dI_a}{dt} = \frac{dI_s}{dt} = \frac{dQ}{dt} = \frac{dQ_n}{dt} = \frac{dR_p}{dt} = \frac{dR_f}{dt}$$

Suppose $\Gamma = \{(S, H_u, H_a, I_a, I_S, Q, Q_n R_P, R_f) \in \mathbb{R}^9 : S > 0, H_u > 0, H_a > 0, I_a > 0, I_S > 0, Q > 0, Q_n > 0, R_P > 0, R_f > 0\}$, then the solution set $\{S_h, E_h, I_h, T_h, R_h, E_v, L_v, P_v, S_v, I_v\}$ is positive for all $t \geq 0$.

Proof:

Observe that,

$$\frac{dH_u}{dt} = T_2 H_u - \mu H_u - n\delta H_u - (1-n)\delta H_u \geq -(\mu + n + (1-n)\delta)H_u$$

This implies

$$\frac{dH_u}{dt} \geq -(\mu + n + (1-n)\delta)H_u$$

From where,

$$H_u(t) \geq H_u(0)\mathrm{e}^{-(\mu+n+(1-n)\delta)t} \tag{15}$$

and

$$\frac{dH_a}{dt} = T_1 H_a - \mu H_a - b_1 H_a \geq -(\mu + b_1)H_a$$

That is

$$H_a(t) \geq H_a(0)e^{-(\mu+b_1)t} \tag{16}$$

And then

$$\frac{dS}{dt} = A + b_1 S Q_n + \eta R_p - \mu S - T_1 H_a - T_2 H_u - u_1 w S \geq -(\mu + u_1 w)S - T_1 H_a - T_2 H_u \tag{17}$$

$$S(t) \geq \left(S_0 + \frac{T_1 H_a(0)\left(1 - e^{(-(b_1 - u_1 w)t)}\right)}{u_1 w - b_1} + \frac{T_2 H_u(0)\left(1 - e^{-(u_1 w - n - (1-n)\delta)t}\right)}{(u_1 w - n - (1-n)\delta)}\right)e^{-(\mu + u_1 w)t}$$

It should be noted that

$$0 < \exp(-(b_1 - u_1 w)t), \exp(-(u_1 w - n - (1-n)\delta)t), \exp(-(\mu + u_1 w)t) \leq 1$$

Thus,

$$S(t) \geq 0 \; \forall \; t \tag{18}$$

Similar procedures revealed that $, E_h(t) > 0, I_h(t) > 0, T_h(t) > 0, R_h(t) > 0, E_v(t) > 0, L_v(t) > 0, P_v(t) > 0, S_v(t) > 0, I_v(t) > 0.$ Hence by the condition of the theorem, the solution set $\{S_h, E_h, I_h, T_h, R_h, E_v, L_v, P_v, S_v, I_v\}$ is positive for all $t \geq 0$

Equilibrium States

The equilibrium point of the system denotes a time when the rate of change of the population is zero. In this case, we set

$$\frac{dS}{dt} = \frac{dH_u}{dt} = \frac{dH_a}{dt} = \frac{dI_a}{dt} = \frac{dI_s}{dt} = \frac{dQ}{dt} = \frac{dQ_n}{dt} = \frac{dR_p}{dt} = \frac{dR_f}{dt} = 0$$

The Disease-Free Equilibrium (DFE)

At disease free equilibrium, $H_u = I_s = I_a = 0$, thus system of the equation becomes

$$\begin{aligned}
\Lambda + b_1 S Q_n + \eta R_p - \mu S - T_1 H_a - u_1 w S &= 0 \\
T_1 H_a - \mu H_a - b_1 H_a &= 0 \\
-T_3 Q - T_4 Q_n &= 0 \\
Q_n &= 0 \\
b_2 H_a - (\mu + \alpha) Q - T_5 R_p - T_6 R_f &= 0 \\
-b_1 S Q_n - (1-\gamma) Q_n - \gamma Q_n &= 0 \\
-b_1 S Q_n - (1-\gamma) Q_n - \gamma Q_n &= 0 \\
T_5 Q + \rho R_f + (1-\gamma) Q_n - (\eta + \mu) R_p &= 0 \\
u_1 w S + T_6 Q + \gamma Q_n - (\rho + \mu) R_f &= 0
\end{aligned}$$

Solving the above system, we have Disease free equilibrium (DFE)

$$\begin{aligned}
&\left(S, H_u, H_a, I_a, I_S, Q, Q_n, R_p, R_f\right) \\
&= \left(\frac{\Lambda}{(\mu + u_1 w)}, 0, 0, 0, 0, 0, 0, 0, 0\right)
\end{aligned}$$

The Endemic Equilibrium (EE)

To obtain the endemic equilibrium, we solve the system of equation

$$0 = A + b_1 S Q_n + \eta R_p - \mu S - T_1 H_a - T_2 H_u - u_1 w S \tag{19}$$

$$0 = T_2 H_u - \mu H_u - n\delta H_u - (1-n)\delta H_u \tag{20}$$

$$0 = T_1 H_a - \mu H_a - b_2 H_a \tag{21}$$

$$0 = n\delta H_u - \mu\alpha I_s - T_3 I_s - T_4 I_s \tag{22}$$

$$0 = (1-n)\delta H_u - T_7 I_a - \mu I_a - \gamma(1 + u_2\tau) I_a \tag{23}$$

$$0 = b_2 H_a + T_3 I_s - (\mu + \alpha) Q - T_5 Q - T_6 Q \tag{24}$$

$$0 = T_7 I_a + T_4 I_s - b_1 S Q_n - (1-n)\gamma Q_n - \gamma n Q_n - \mu Q_n \tag{24}$$

$$0 = \gamma(1 + u_2\tau) I_a + T_5 Q + \rho R_f + (1-\gamma) Q_n - (\eta + \mu) R_p \tag{26}$$

$$0 = u_1 w S + T_6 Q + \gamma Q_n - (\rho + \mu) R_f \tag{27}$$

From equation (2) and (3) respectively,

$$H_u(t) = 0 \; and \; H_a(t) = 0 \tag{28}$$

Solving the equations, the critical points are

$$\left[S(t) = \frac{\Lambda(\eta+\mu)(\mu+\rho)}{\mu\left((u_1 w+\mu)(\eta+\mu+\rho)+\eta\rho\right)},\right.$$
$$Q(t) = 0, Qn(t) = 0, Hu(t) = 0,$$
$$Rp(t) = \frac{\Lambda\rho u_1 w}{\mu\left((u1w+\mu)(\eta+\mu+\rho)+\eta\rho\right)},$$
$$Ha(t) = 0, Da(t) = 0, Ds(t) = 0,$$
$$\left.Rf(t) = \frac{\Lambda u1w(\eta+\mu)}{\mu\left((u1w+\mu)(\eta+\mu+\rho)+\eta\rho\right)}\right]$$

$$\left[S(t) = -\frac{\gamma+\mu}{b_1}, Q(t) = 0,\right.$$
$$Qn(t) = \frac{d_1 + \Lambda(\mu+\rho)b_1(\eta+\mu)+d_2}{d_3},$$
$$Hu(t) = 0, Ha(t) = 0, Da(t) = 0, Ds(t) = 0,$$
$$Rp(t) = -\frac{d_4 + \Lambda b1\gamma\mu n - \Lambda b1\gamma(\mu+\rho) - d_5}{d_3},$$
$$\left.Rf(t) = \frac{\Lambda b1\gamma n(\eta+\mu)+d_6(\gamma+\mu)}{d_3}\right]$$

Where $(\mu\eta + (\eta+\mu+\rho)\gamma)\mu u1w + \mu^2(\mu+\rho)u_1 w = d_1$

$$(\mu+\rho)\eta\gamma\mu + (\mu+\rho)\mu^2(\eta+\gamma+\mu) = d_2$$
$$b_1\mu\left(\eta\gamma n + (\eta+\gamma+\mu)(\mu+\rho)\right) = d_3$$
$$\mu(\gamma+\mu)(\gamma n(u1w+\mu)+\rho u1w) = d_4$$
$$(\gamma\mu u1w + \gamma\mu + \rho)\mu(\gamma+\mu) = d_5$$
$$\gamma\mu n(u1w+\eta+\mu) - (\eta+\gamma+\mu)\mu u1w = d_6$$

It should be noted that the second critical point is not feasible as $S(t) \not< 0$

The Basic Reproduction Number (BRN)

The epidemiologic concept of R naught (R_0) is much in the news of late. This number, the basic reproduction number, is being used to calculate transmissibility of infectious diseases and is a key part of the discussion on effective strategies of control and prevention of diphtheria. The basic reproduction number, is one of the most fundamental and often-used metrics for the study of the way a disease spread. The symbol R represents the actual transmission rate of a disease and stands for reproduction. Naught, or zero, stands for the zeroth generation (patient zero). It refers to the first documented patient infected by a disease in an epidemic. R0 is an indicator of the contagiousness or transmissibility of infectious and parasitic agents and represent the number of new infections estimated to stem from a single case in a population that has never seen the disease before. If the R0 is 2, then one person is expected to infect, on average, two new people (Anastassopoulou et al., 2020).

The Next Generation Matrix

The Next Generation Matrix is a mathematical tool used in epidemiology to calculate the basic reproduction number (R_0) or the effective reproduction number (R_t) of infectious diseases. It helps epidemiologists and researchers understand the dynamics of disease transmission within a population.

Now, from

$$\frac{dH_u}{dt} = T_2 H_u - \mu H_u - n\delta H_u - (1-n)\delta H_u \quad (29)$$

$$\frac{dH_a}{dt} = T_1 H_a - \mu H_a - b_2 H_a \quad (30)$$

$$\frac{dI_s}{dt} = n\delta H_u - \mu\alpha I_s - T_3 I_s - T_4 I_s \quad (31)$$

$$\frac{dI_a}{dt} = (1-n)\delta H_u - T_7 I_a - \mu I_a - \gamma(1+u_2\tau)I_a \quad (32)$$

$$\frac{dQ}{dt} = b_2 H_a + T_3 I_s - (\mu+\alpha)Q - T_5 Q - T_6 Q \quad (33)$$

$$\frac{dQ_n}{dt} = T_7 I_a + T_4 I_s - b_1 S Q_n - (1-n)\gamma Q_n - \gamma n Q_n - \mu Q_n \quad (34)$$

$$F = \frac{d}{dX}\begin{pmatrix} T_2 H_u \\ T_1 H_a \\ n\delta H_u \\ (1-n)\delta H_u \\ b_2 H_a + T_3 I_s \\ T_7 I_a + T_4 I_s \end{pmatrix} = \begin{pmatrix} T_2 & 0 & 0 & 0 & 0 & 0 \\ 0 & T_1 & 0 & 0 & 0 & 0 \\ n\delta & 0 & 0 & 0 & 0 & 0 \\ (1-n)\delta & 0 & 0 & 0 & 0 & 0 \\ 0 & b_2 & T_3 & 0 & 0 & 0 \\ 0 & 0 & T_7 & T_4 & 0 & c_0 \end{pmatrix}$$

$$V = \frac{d}{dx}\begin{pmatrix} \mu H_u + n\delta H_u + (1-n)\delta H_u \\ \mu H_a + b_2 H_a \\ \mu\alpha I_s + T_3 I_s + T_4 I_s \\ (1-n)\delta H_u + \big(T_7 + \mu + \gamma(1+u_2\tau)\big) I_a \\ \big((\mu+\alpha) + T_5 + T_6\big) Q \\ (b_1 S + \gamma + \mu) Q_n \end{pmatrix} = \begin{pmatrix} c_1 & 0 & 0 & 0 & 0 & 0 \\ 0 & \mu + b_2 & 0 & 0 & 0 & 0 \\ 0 & 0 & c_2 & 0 & 0 & 0 \\ (1-n)\delta & 0 & 0 & c_3 & 0 & 0 \\ 0 & b_2 & T_3 & c_4 & 0 & 0 \\ 0 & 0 & T_4 & T_7 & 0 & c_0 \end{pmatrix}$$

$$F := \begin{bmatrix} T_2 & 0 & 0 & 0 & 0 & 0 \\ 0 & T_1 & 0 & 0 & 0 & 0 \\ n\delta & 0 & 0 & 0 & 0 & 0 \\ (1-n)\delta & 0 & 0 & 0 & 0 & 0 \\ 0 & b_2 & T_3 & 0 & 0 & 0 \\ 0 & 0 & T_7 & T_4 & 0 & 0 \end{bmatrix}$$

$$V = \begin{bmatrix} 0 & -c[5] & -c[6] & -c[7] & c[8] & 0 \\ 0 & \frac{1}{\mu + b_2} & 0 & 0 & 0 & 0 \\ 0 & 0 & \frac{1}{c_2} & 0 & 0 & 0 \\ 0 & -c[9] & -\frac{T_3}{c_2 c_4} & 0 & \frac{1}{c_4} & 0 \\ -\frac{c_5}{\mu^2} & c[10] & c[11] & -c[12] & -c[13] & \frac{1}{\mu} \\ \frac{1}{\mu} & c[14] & c[15] & c[16] & -c[17] & 0 \end{bmatrix}$$

$$V^{-1} = \begin{bmatrix} 0 & -c_5 & -c_6 & -c_7 & c_8 & 0 \\ 0 & \frac{1}{\mu + b_2} & 0 & 0 & 0 & 0 \\ 0 & 0 & \frac{1}{c_2} & 0 & 0 & 0 \\ 0 & -c_9 & -\frac{T_3}{c_2 c_4} & 0 & \frac{1}{c_4} & 0 \\ -\frac{c_5}{\mu^2} & c_{10} & c_{11} & -c_{12} & -c_{13} & \frac{1}{\mu} \\ \frac{1}{\mu} & c_{14} & c_{15} & c_{16} & -c_{17} & 0 \end{bmatrix}$$

Therefore,

$$FV^{-1} = \begin{bmatrix} 0 & -c_{18} & -c_{19} & -c_{20} & c_{21} & 0 \\ 0 & c_{22} & 0 & 0 & 0 & 0 \\ 0 & -c_{23} & -c_{24} & -1 & c_{25} & 0 \\ 0 & -c_{26} & -c_{27} & 1 & c_{28} & 0 \\ 0 & c_{29} & \frac{T_3}{c_2} & 0 & 0 & 0 \\ 0 & -c_{30} & c_{31} & 0 & \frac{T_4}{c_4} & 0 \end{bmatrix}$$

where

$$c_1 = \mu + \delta, c_2 = \mu\alpha + T_3 + T_4,$$

$$c_3 = T_7 + \mu + \gamma(1 + u_2\tau),$$

$$c_4 = (\mu + \alpha) + T_5 + T_6,$$

$$c_0 = \frac{\Lambda(\eta + \mu)(\mu + \rho)b_1}{\mu\big((u_1 w + \mu)(\eta + \mu + \rho) + \eta\rho\big)} + \gamma + \mu$$

$$c_5 = \frac{b_2 c_3}{(\mu + b_2)c_4(-1 + n)\delta},$$

$$c_6 = \frac{T_3 c_3}{c_2 c_4(-1 + n)\delta}, c_7 = \frac{1}{(-1 + n)\delta},$$

$$c_8 = \frac{c_3}{c_4(-1 + n)\delta}, c_9 = v, c_{10} = v,$$

$$c_{11} = \frac{(\delta\mu n T_3 T_7 - \delta\,\mu n T_4 c_4 - \delta\mu T_3 T_7 + \delta\,\mu\,T_4 c_4 - T_3 c_1 c_3 c_5)}{c_2 c_4(n-1)\delta\,\mu^2},$$

$$c_{12} = \frac{c_5 c_1}{(-1 + n)\delta\,\mu^2},$$

$$c_{13} = \frac{\delta\,\mu\,n\,T_7 - \delta\,\mu T_7 - c_1 c_3 c_5}{c_4(-1 + n)\delta\,\mu^2},$$

$$c_{14} = \frac{b_2 c_3 c_1}{(\mu + b_2)c_4(-1 + n)\delta\,\mu},$$

$$c_{15} = \frac{T_3 c_3 c_1}{c_2 c_4(-1 + n)\delta\,\mu},$$

$$c_{16} = \frac{c_1}{(-1 + n)\delta\,\mu}, c_{17} = \frac{c_3 c_1}{c_4(-1 + n)\delta\,\mu},$$

$$c_{18} = \frac{T_2 b_2 c_3}{(\mu + b_2)c_4(-1 + n)\delta},$$

$$c_{19} = \frac{T_2 T_3 c_3}{c_2 c_4(-1 + n)\delta},$$

$$c_{20} = \frac{T_2}{(-1 + n)\delta}, c_{21} = \frac{T_2 c_3}{c_4(-1 + n)\delta},$$

$$c_{22} = \frac{T_1}{\mu + b_2}, c_{23} = \frac{n b_2 c_3}{(\mu + b_2)c_4(-1 + n)},$$

$$c_{24} = \frac{n T_3 c_3}{c_2 c_4(-1 + n)}, c_{25} = \frac{n c_3}{c_4(-1 + n)},$$

$$c_{26} = \frac{(1 - n)b_2 c_3}{(\mu + b_2)c_4(-1 + n)},$$

$$c_{27} = \frac{(1 - n)T_3 c_3}{c_2 c_4(-1 + n)},$$

$$c_{28} = \frac{(1 - n)c_3}{c_4(-1 + n)}, c_{29} = \frac{b_2}{\mu + b_2},$$

$$c_{30} = \frac{T_4 b_2}{(\mu + b_2)c_4}, c_{31} = \frac{T_7}{c_2} - \frac{T_4 T_3}{c_2 c_4}$$

Therefore, the eigenvalue corresponds to the basic reproduction number R_0, which is the average number of secondary infections caused by a single infected individual in a fully susceptible population is given by the dominant

eigenvalue
$\Lambda(\eta+\mu)(\mu+\rho)/\mu\big((u_1 w+\mu)(\eta+\mu+\rho)+\eta\rho\big)$

Therefore,

$$R_0=\frac{\Lambda(\eta+\mu)(\mu+\rho)}{\mu\big((u_1 w+\mu)(\eta+\mu+\rho)+\eta\rho\big)}$$

followed, and structure this information as logically as possible.

Results and Discussion

Numerical Solution. The set of system of equations (1)-(9) is solve numerically using rkf45 codes implemented by computational software Maple 2022. The dsolve command with the numeric or type=numeric option and an initial value problem (IVP) finds a numerical solution for our ODE system IVP. The optional equation method=numericmethod (rkf45) is provided, and the Maple command "dsolve" uses that method to obtain the numerical solution.

Model Validation

To validate our computations, it could be observed that equations (2) and (3) are simple first order ode which are

$$\frac{dH_u}{dt}=T_2H_u-\mu H_u-n\delta H_u \\ -(1-n)\delta H_u \qquad (35)$$

$$\frac{dH_a}{dt}=T_1H_a-\mu H_a-b_2H_a \qquad (36)$$

As such, integrating respectively

$$H_u(t)=H_u(0)\exp(-(\mu+\delta-T_2)t) \\ H_a(t)=H_a(0)\exp(-(\mu+b_2-T_1)t) \qquad (37)$$

Comparing the above graphical representation to the one obtained by numerical computations as shown below reveal that the two results are in perfect agreement.

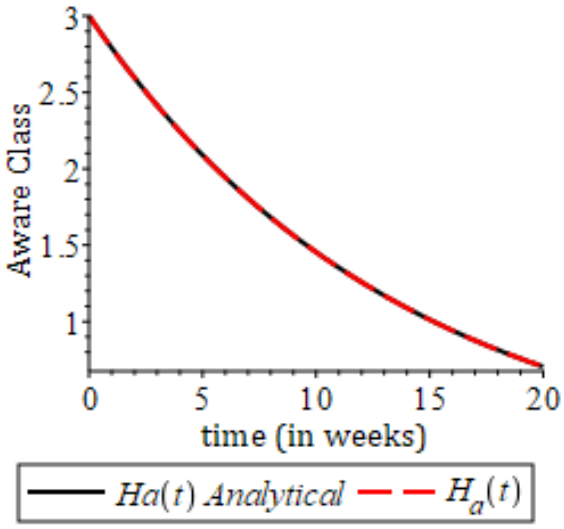

Figure 2. Comparison between Analytical (solid black line) and Numerical (dash red line) solution for aware class ($Ha(t)$)

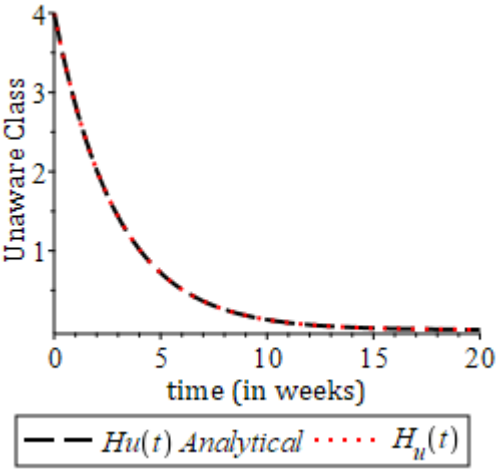

Figure 3. Comparison between Analytical (solid black line) and Numerical (dash red line) solution for Unaware class $Hu(t)$

Parameter Effects on the BRN

From the fact that

$$R_0=\frac{\Lambda(\eta+\mu)(\mu+\rho)}{\mu\big((u_1 w+\mu)(\eta+\mu+\rho)+\eta\rho\big)}$$

The effect of each parameter on R_0 is investigated.

$$\frac{dR_0}{d\Lambda} = \frac{(\eta+\mu)(\mu+\rho)}{\mu(\eta u1w + \mu u1w + \rho u1w + \eta\mu + \eta\rho + \mu^2 + \mu\rho)}$$

$$\frac{\eta\mu + \eta\rho + \mu^2 + \mu\rho}{\mu(\eta u1w + \mu u1w + \rho u1w + \eta\mu + \eta\rho + \mu^2 + \mu\rho)} < 1$$

Implies

$$\eta\mu + \eta\rho + \mu^2 + \mu\rho - \big(\mu(\eta\mu + \eta\rho + \mu^2 + \mu\rho)\big) < \mu(\eta + \mu + \rho)u1w$$

$$\eta\rho\frac{(1-\mu)}{(u1w + \mu - 1)} < (\eta\mu + \mu^2 + \mu\rho)$$

That is

$$\frac{\eta\rho}{(\eta\mu + \mu^2 + \mu\rho)}\frac{(1-\mu)}{(u_1w + \mu - 1)} < 1$$

Also

$$\frac{dR_0}{d\eta} = \frac{\Lambda(\mu+\rho)}{\mu\big((\eta+\mu\ +\rho)u_1w + (\eta+\mu)(\mu+\rho)\big)^2} - \frac{\Lambda(\eta\mu + \eta\rho + \mu^2 + \mu\rho)(u1w + \mu + \rho)}{\mu\big((\eta+\mu\ +\rho)u_1w + (\eta+\mu)(\mu+\rho)\big)^2}$$

Which gives

$$\frac{dR_0}{d\eta} = \frac{\Lambda(\mu+\rho)\Lambda(\eta\mu + \eta\rho + \mu^2 + \mu\rho)(u1w + \mu + \rho)}{\mu\big((\eta+\mu\ +\rho)u_1w + (\eta+\mu)(\mu+\rho)\big)^2}$$

$$\frac{dR_0}{d\mu} = \frac{\begin{pmatrix}\Lambda(\eta+\mu) + \Lambda(\mu+\rho) \\ -\Lambda(\eta+\mu)(\mu+\rho)\big(1 + (u1w + \eta + 2\mu + \rho)\big)\end{pmatrix}}{\mu\big((\eta+\mu\ +\rho)u_1w + (\eta+\mu)(\mu+\rho)\big)^2}$$

$$\frac{dR_0}{d\rho} = \frac{\Lambda(\eta+\mu)}{\mu\big((\eta+\mu\ +\rho)u_1w + (\eta+\mu)(\mu+\rho)\big)^2} - \frac{\Lambda(\eta\mu + \eta\rho + \mu^2 + \mu\rho)(u1w + \eta + \mu)}{\mu\big((\eta+\mu\ +\rho)u_1w + (\eta+\mu)(\mu+\rho)\big)^2}$$

Which implies

$$\frac{dR_0}{d\rho} = \frac{\Lambda(\eta+\mu) - \Lambda(\eta\mu + \eta\rho + \mu^2 + \mu\rho)(u1w + \eta + \mu)}{\mu\big((\eta+\mu\ +\rho)u_1w + (\eta+\mu)(\mu+\rho)\big)^2}$$

$$\frac{dR_0}{du_1} = -\frac{\Lambda(\eta\mu + \eta\rho + \mu^2 + \mu\rho)(\eta w + \mu w + \rho w)}{\mu\big((\eta+\mu\ +\rho)u_1w + (\eta+\mu)(\mu+\rho)\big)^2}$$

$$\frac{dR_0}{dw} = -\frac{\Lambda(\eta\mu + \eta\rho + \mu^2 + \mu\rho)(\eta u_1 + \mu u1 + \rho u1)}{\mu\big((\eta+\mu\ +\rho)u_1w + (\eta+\mu)(\mu+\rho)\big)^2}$$

Sensitivity Analysis

Now examine the sensitivity of the parameters on Basic reproduction number. we analyze the

sensitivity of the parameters of the basic reproduction
number (R_0). We employ the approach used by Kizito and Tumwiine (2018) to compute the sensitivity of the parameters of R_0. The sensitivity of a parameter, say μ, of R_0 is defned as

$$\varsigma_{\mu}^{R_0} = \frac{\partial R_0}{\partial \mu} \times \frac{\mu}{R_0}. \quad (38)$$

The sensitivity indices of the parameters are presented as follows:

$$\varsigma_{\Lambda}^{R_0} = \frac{\partial R_0}{\partial \Lambda} \times \frac{\Lambda}{R_0} = 1$$

$$\varsigma_{\eta}^{R_0} = \frac{\partial R_0}{\partial \eta} \times \frac{\eta}{R_0}.$$
$$= \frac{u_1 w \rho \eta}{\begin{pmatrix}(wu_1 + \mu + \rho)\eta \\ +(\mu + \rho)(wu_1 + \mu)\end{pmatrix}(\eta + \mu)}$$

$$\varsigma_{\mu}^{R_0} = \frac{\partial R_0}{\partial \mu} \times \frac{\mu}{R_0} = -$$
$$\frac{\begin{pmatrix}\mu^4 + 2(\eta + \rho)\mu^3 + 2\eta\rho\mu^2 \\ +2\eta\rho(wu_1 + \eta + \rho)\mu + (\eta + \rho)\mu^2 \\ +\rho(wu_1(\eta + \rho) + \rho\eta)\eta\end{pmatrix}}{\left((\mu + \rho)\begin{pmatrix}\mu^2 + (wu_1 + \eta + \rho)\mu \\ +(wu_1 + \rho)\eta + \rho w u_1\end{pmatrix}(\eta + \mu)\right)} < 0$$

$$\varsigma_{\rho}^{R_0} = \frac{\partial R_0}{\partial \rho} \times \frac{\rho}{R_0}$$
$$= \frac{u_1 w \rho \eta}{(\mu + \rho)\begin{pmatrix}(wu_1 + \eta + \mu)\rho \\ +(\eta + \mu)(wu_1 + \mu)\end{pmatrix}}$$

$$\varsigma_{w}^{R_0} = \frac{\partial R_0}{\partial w} \times \frac{w}{R_0}$$
$$= -\frac{u_1(\eta + \mu + \rho)w}{(wu_1 + \mu)(\eta + \mu + \rho) + \eta\rho}$$
$$< 0$$

$$\varsigma_{u_1}^{R_0} = \frac{\partial R_0}{\partial u_1} \times \frac{u_1}{R_0}$$
$$= -\frac{u_1(\eta + \mu + \rho)w}{(wu_1 + \mu)(\eta + \mu + \rho) + \eta\rho} < 0$$

Table 2. Table of Sensitivity Index

Parameter	Rate of change	Sensitivity
Λ	5.668934240	1
ρ	0.52105784	0
η	-1.0×10^{-9}	-0.71×10^{-10}
w	−0.3213681542	−0.0227
u_1	−12.85472617	−0.0227
μ	−32.13681543	−.9773

The analysis revealed that the positively sensitive parameter of the basic reproduction number, R_0, is the recruitment rate (Λ) into the susceptible class, Thus, reducing the number of susceptible individuals, effectively restricting infected humans from adding to the pathogen population, and ensuring that protected individuals remain protected can greatly lower the value of the basic reproduction number (R_0) and thereby increasing the stability of the disease-free equilibrium. Increasing the value of the positively sensitive parameter has the effect of increasing the value of the basic reproduction number (R_0), which is not a desired condition. Whereas, the negatively sensitive parameters are the mortality rate (μ), Vaccine coverage (u_1), rate of losing immunity (ρ), vaccine effectiveness (w) and rate of regaining susceptibility (η). Increasing the values of these negatively sensitive parameters, reduces the value of the basic reproduction number (R0), which is the desired condition.

Discussions

In this section, we provide the analytical solutions for the system of ode. In order to analyze the outcome very succinctly, we explore the effect of variation of each of the parameters and displayed the graphs for corresponding discussion.

A population-time graph represents the change in a population over time, with the x-axis indicating time and the y-axis showing population size as seen in Fig. 4. An upward-sloping trend indicates population growth, while a downward slope shows a decline. Fluctuations in the graph may suggest varying birth rates, death rates, or migration patterns. Exponential growth is depicted by an upward curve, whereas a leveling off indicates a carrying capacity or logistic growth. These graphs are used in various fields, including ecology, demography, and public health, to understand and manage population dynamics. As shown in Fig. 5, the recruitment rate, Λ represents the rate at which new individuals enter a particular class, such as the susceptible class in epidemiological models. Directly, an increase in Λ generally leads to more individuals entering the susceptible class while a decrease in Λ results in fewer individuals entering the susceptible class. Indirectly, changes in Λ can affect downstream variables in the system. For example, if the system involves transitions from the susceptible class to other classes, an increased recruitment rate can lead to more individuals transitioning, affecting overall system dynamics which could impact the rate of spread in an epidemiological context, increasing the chances of transmission due to a larger susceptible population. Also, the equilibrium state of the system can be influenced by the recruitment rate reason being that if the recruitment rate is high, the system may reach a new equilibrium with a larger susceptible population thereby affecting stability. Treatment success as seen in Fig. 6 and 7 reduces the rate at which susceptible individuals become infected, lowering transmission risk. By effectively treating infected individuals, the infectious period is shortened, resulting in fewer people in the not-quarantined class (those who aren't isolated). This reduction in infection rates and quicker recovery means fewer transitions from the susceptible to the infected class, ultimately slowing disease spread. Successful treatment also increases the recovered population, contributing to herd immunity and reducing overall transmission.

From Fig 8 and 9 respectively, the rate of regaining susceptibility profoundly impacts both the "Recovered with partial immunity" and susceptible classes in epidemiological models. For the "Recovered with partial immunity" class, a slower rate means individuals retain partial immunity for longer periods, acting as a natural brake on disease transmission and aiding epidemic control by reducing the pool of susceptible individuals. However, this also prolongs the period during which they remain vulnerable to reinfection.

Meanwhile, for the susceptible class, a slower rate translates to a delayed replenishment of individuals who are fully susceptible to the disease, slowing down the rate of new infections and potentially extending the epidemic duration.

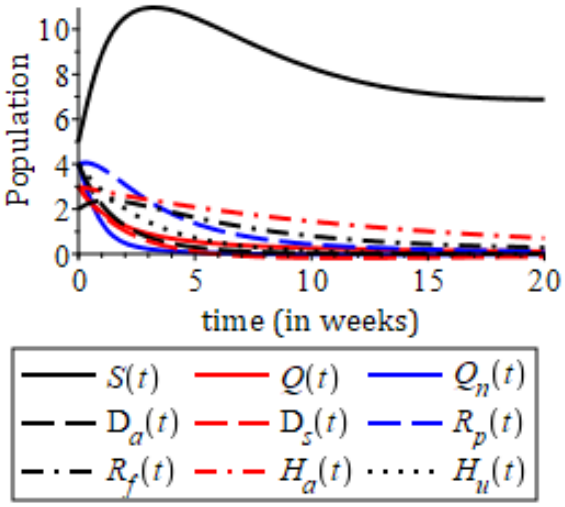

Figure 4. Model Population Time Graph

Consequently, understanding and accurately modeling the rate of regaining susceptibility is crucial for assessing disease dynamics and designing effective intervention strategies to mitigate the spread of infectious diseases. It could be observed that as the rate increases,

recovered with partial immunity declines while susceptible class is enhanced.

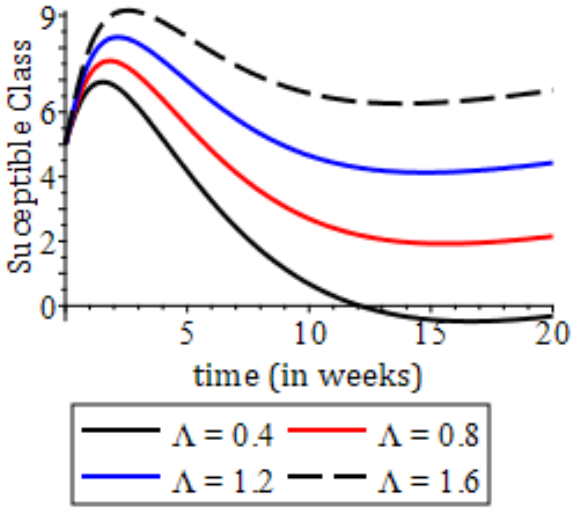

Figrky 5. Impact of Recruitment Rate of the Susceptible Class

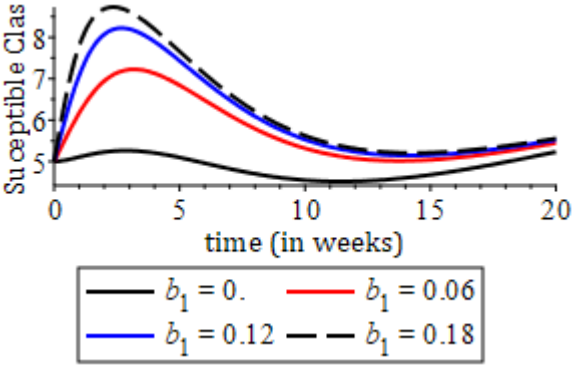

Figure 6. Effect Treatment Success Probability on the Suceptible Class

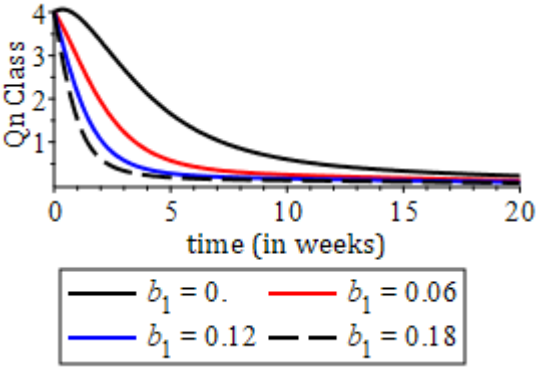

Figure 7 Effect Treatment Success Probability on Quarantined Population

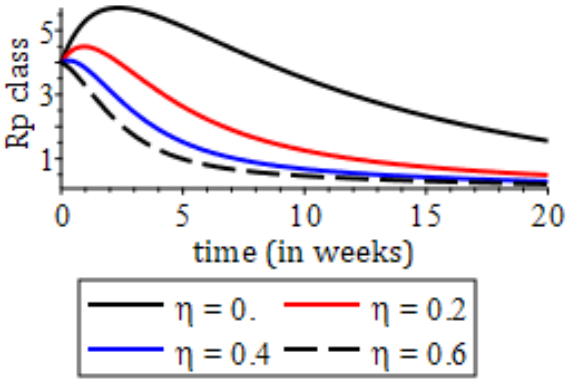

Fig. 8 Impact of Rate of Regaining Susceptibility on Recovered with Partial Immunity Class

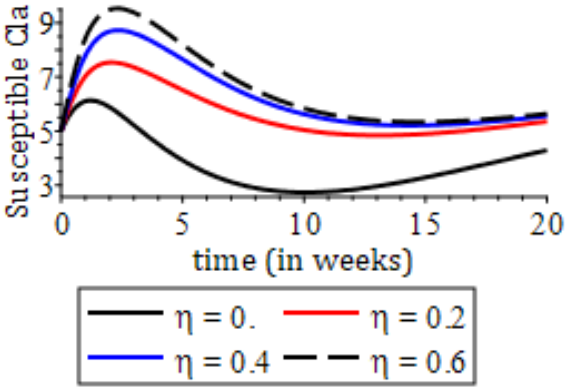

Figure 9. Impact of Rate of Regaining Susceptibility on Susceptible Class

The impact of the progression rate from symptomatically infected to not quarantined is reflected in the speed at which individuals transition from being actively contagious within the community, potentially leading to increased transmission rates and challenges in containment efforts as displayed in Fig 10. While in Fig 11, the impact of isolation rate on the symptomatically infected population directly influences the effectiveness of containing disease transmission within the community, potentially reducing the spread of infection and mitigating the burden on healthcare systems. The effect of exposure rate on the exposed but not yet infectious class determines the pace at which individuals transition to becoming

infectious, influencing the overall rate of disease transmission within the population. This, as displayed in Fig 12 is observed to enhanced the uninfected exposed subclass of the population while, the reverse is the observed trend in susceptible class as shown in Fig 13. In such case, the effect of exposure rate on the susceptible class dictates the speed at which individuals become exposed to the infectious agent, impacting the rate of new infections and the overall progression of the epidemic.

From Figs. 14 and 15, the influence of latency on both susceptible and incubating infections are displayed. The latency period indirectly affects the susceptible class by determining the duration individuals remain in this state before being exposed to the infectious agent. A shorter latency period means individuals transition more quickly from being susceptible to being exposed, potentially leading to a faster rate of new infections within the population. For individuals in the incubating infections class, the latency period directly determines the duration between exposure to the pathogen and the onset of infectiousness. A longer latency period means individuals spend more time in the incubating stage before becoming infectious, impacting the timing and pace of disease transmission within the population. Additionally, the duration of the latency period can affect the effectiveness of control measures, as it influences the window of time during which individuals may be infectious but not yet showing symptoms.

The progression rate from exposed to quarantined determines how quickly individuals identified as exposed are isolated from the general population, Fig 16. A higher progression rate facilitates prompt quarantine of exposed individuals, which helps prevent them from potentially infecting others during the latent period of the disease. This rapid isolation is crucial for breaking chains of transmission and reducing the overall spread of the infection within the community. Additionally, efficient quarantine measures can alleviate strain on healthcare systems by reducing the number of severe cases requiring medical attention, thus ensuring resources are available for those who need them most. Therefore, the progression rate from exposed to quarantined plays a critical role in controlling disease transmission and managing the impact of an epidemic. In Fig 17, we displayed the impact of wanning immunity rate on recovered with full immunity class. The waning immunity rate directly influences the duration of protection individuals in the Recovered with full immunity class have against reinfection. A faster waning immunity rate means individuals lose their immunity more quickly, leaving them susceptible to contracting the disease again. This can lead to an increase in the number of previously immune individuals becoming susceptible, potentially contributing to resurgence or secondary outbreaks of the disease over time. Moreover, the waning immunity rate impacts public health strategies, as it informs decisions regarding vaccination schedules and booster doses to maintain population-level immunity. Therefore, understanding the dynamics of waning immunity is crucial for long-term epidemic control and vaccine policy planning.

The impact of the recovery rate with treatment to partial immunity on both the Quarantine and partial recovery classes is significant and nuanced. A higher recovery rate with treatment among individuals in the Quarantine class accelerates their transition to partial immunity, reducing the duration they remain isolated and potentially contagious, Fig 18 and 19. This can alleviate the burden on quarantine facilities and healthcare systems while contributing to the development of herd immunity. However, if the recovery rate is too rapid, there's a risk of premature release from quarantine, potentially leading to continued transmission. Meanwhile, for individuals in the partial recovery class, a higher recovery rate with treatment means a quicker transition to full recovery, reducing the duration they remain partially immune. This may affect the dynamics of disease transmission and the overall effectiveness of public health interventions aimed at controlling the spread of infectious diseases. Therefore, optimizing the recovery rate with treatment is crucial for balancing the need to alleviate the burden on healthcare systems with the imperative of minimizing transmission risks.

Fig. 20 and 21 explains the impact of the recovery rate with treatment to full immunity on both the partial recovery and quarantine classes is pivotal for epidemic management. A higher recovery rate with treatment among individuals in the partial recovery class accelerates their transition to full immunity, reducing the duration they remain partially immune and potentially susceptible to reinfection. This may contribute to building population-level immunity and slowing disease transmission. However, if the recovery rate is too rapid, there's a risk of individuals being prematurely released from partial recovery, potentially leading to relapse or continued transmission. Conversely, in the quarantine class, a higher recovery rate means individuals are more swiftly removed from quarantine upon full recovery, reducing the burden on quarantine facilities and enabling resources to be reallocated efficiently. However, if the recovery rate is too slow, it prolongs the duration of quarantine, potentially straining healthcare systems and impeding epidemic control efforts. Therefore, striking the right balance in the recovery rate with treatment to full immunity is crucial for optimizing both individual health outcomes and epidemic containment strategies.

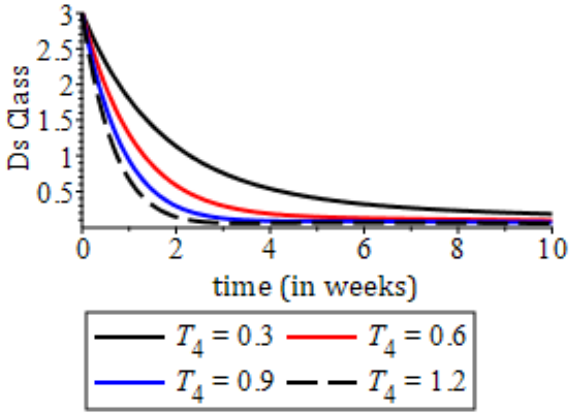

Figure 10. Impact of Progression Rate from Symptomatically Infected to not Quarantined

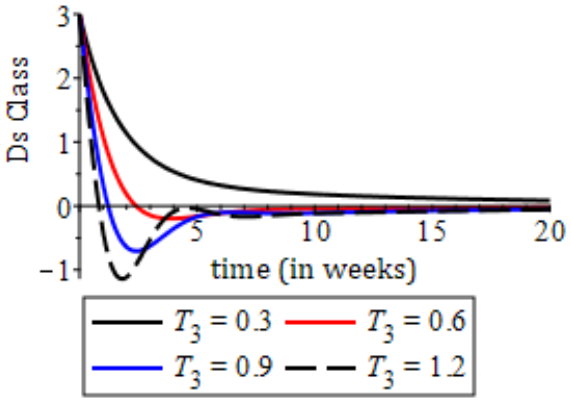

Figure 11. Impact of Isolation Rate on Symptomatically Infected Population

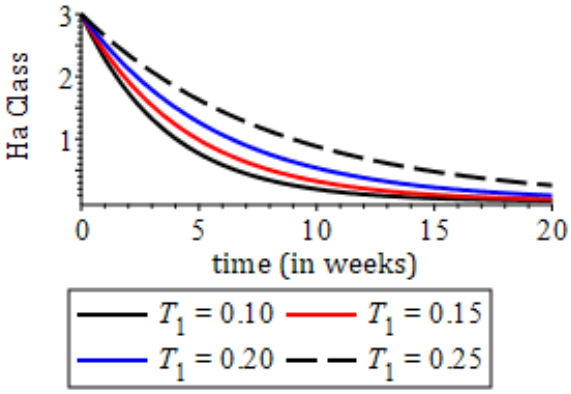

Figure 12. Effect of Exposure Rate on the Exposed but not yet Infectious Class

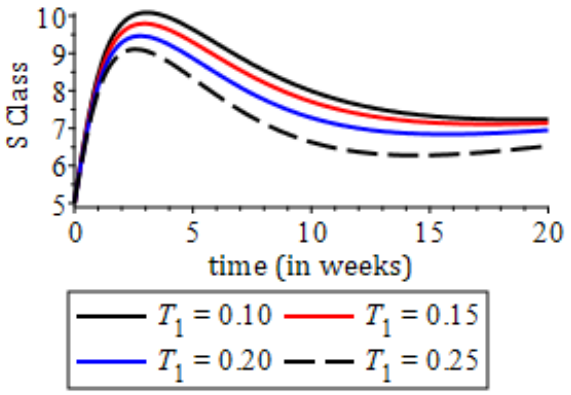

Fig 13: Effect of exposure rate of the susceptible Class

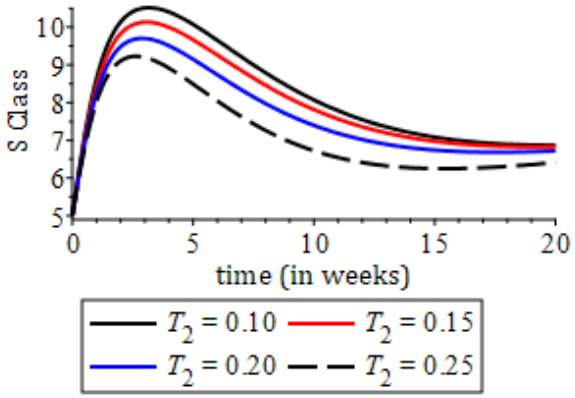

Figure 14. Imapct of Latency Rate on the Suceptible Class

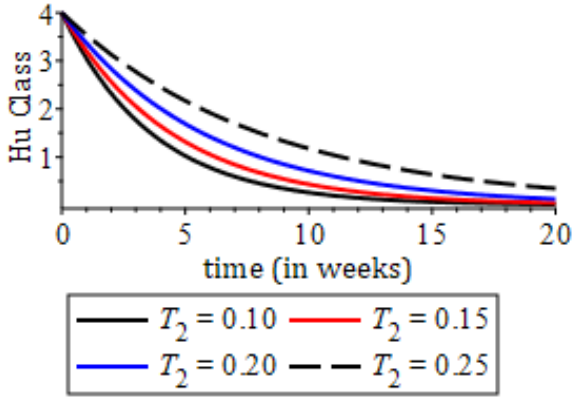

Figure 15. Influence of Latency Rate on ***Hu*** Class

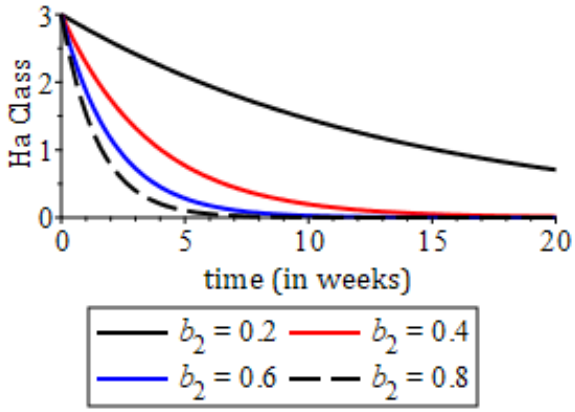

Figure 16. Impact of Progression Rate from Exposed to qQuarantined

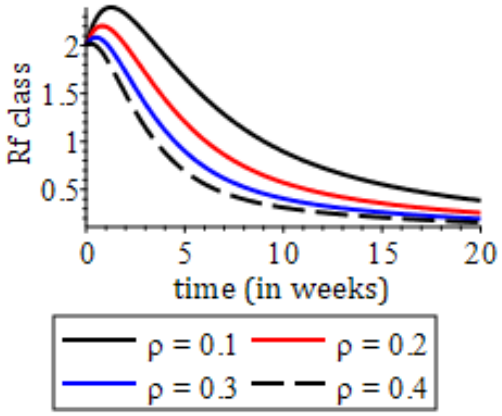

Figure 17. Impact of Wanning Immunity Rate on Recovered with Full Immunity Class

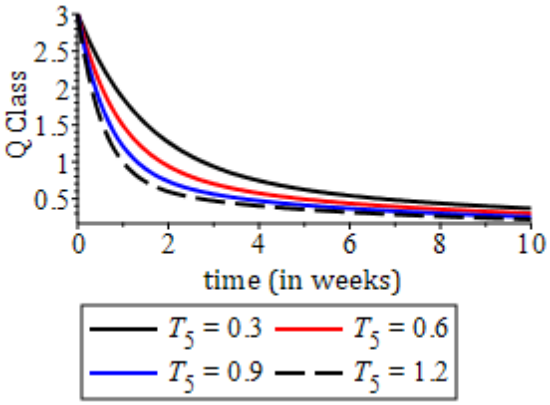

Figure 18. Impact of Recovery Rate with Treatment to Partial Smmunity on Quarantine Class

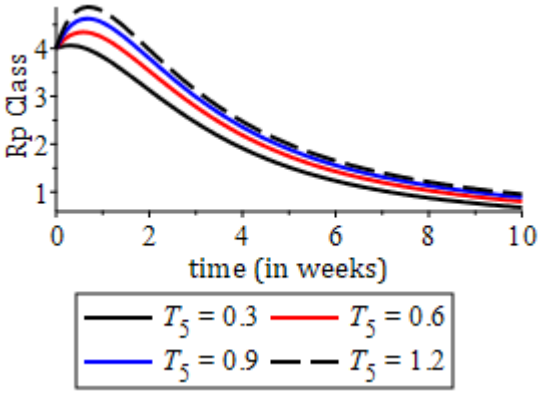

Figure 19. Impact of Recovery Rate with Treatment to Partial Immunity on Partial Recovery Class

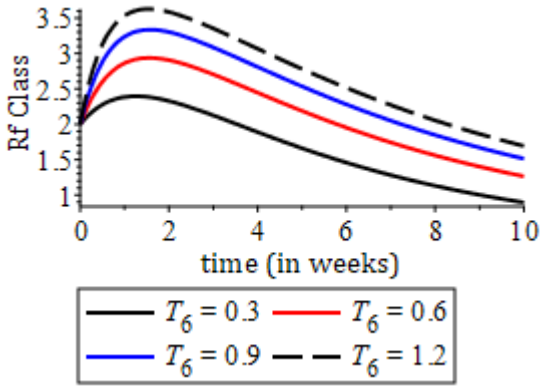

Figure 2.: Impact of Recovery Rate with Treatment to Full Immunity on Partial Recovery

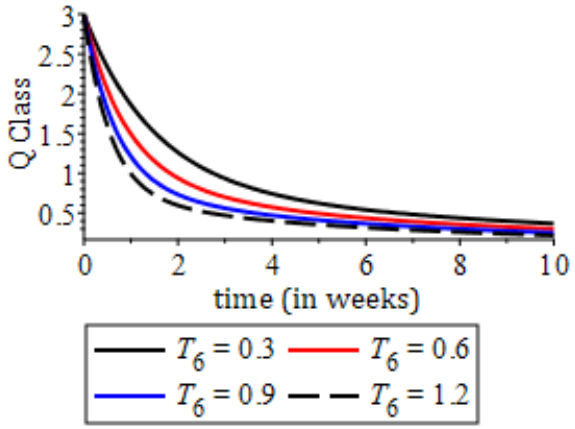

Figure 21. Impact of Recovery Rate with Treatment to Full Immunity on Quarantine Class

Conclusion

This mathematical analysis of the dynamics of diphtheria transmission and the effectiveness of diphtheria anti-toxin (DAT) as a control measure was studied in this paper. The dynamics of disease spread, as depicted in population-time graphs and influenced by factors such as recruitment rate, loss of immunity, treatment success, regaining susceptibility, latency rate, natural death rate, exposure rate, and vaccination coverage, underscore the complexity of managing and controlling infectious diseases like diphtheria. While successful treatment and vaccination coverage can mitigate transmission risk and bolster herd immunity, factors such as loss of immunity and exposure rate can challenge these efforts by increasing the susceptible population and fostering conditions for outbreaks. Public health interventions must navigate these interconnected variables to effectively control disease spread, emphasizing the need for comprehensive strategies that address not only treatment and vaccination but also population dynamics and immunity management. The following were deduced from this work:

Population-time graphs depict changes in population size over time, with trends indicating growth, decline, or fluctuations due to factors like birth rates, death rates, or migration patterns.

The recruitment rate (Λ) represents the rate at which new individuals enter the susceptible class, affecting both the susceptible class size and downstream variables, impacting disease spread and equilibrium states.

Treatment success reduces the rate at which susceptible individuals become infected, leading to fewer transitions to the infected class, ultimately slowing disease spread and increasing the recovered population.

The rate of regaining susceptibility affects the duration of partial immunity in the recovered class and the replenishment of the susceptible class, influencing disease transmission dynamics and epidemic duration.

The progression rate from symptomatically infected to not quarantined impacts transmission rates and containment efforts, while the isolation rate directly influences disease transmission containment within the community.

Exposure rate affects transitions to infectiousness and new infections, influencing epidemic progression.

Latency period duration impacts transitions from susceptibility to exposure and the timing of infectiousness onset, affecting disease transmission and control measures' effectiveness.

The progression rate from exposed to quarantined is crucial for timely isolation, preventing further transmission, and reducing strain on healthcare systems.

Waning immunity rate affects the duration of protection against reinfection in the recovered class, impacting disease resurgence and vaccine policy decisions.

The recovery rate with treatment to partial immunity affects transitions from quarantine to partial immunity and from partial recovery to full immunity, balancing containment efforts and transmission risks.

The recovery rate with treatment to full immunity influences transitions to full immunity from both partial recovery and quarantine, optimizing individual health outcomes and epidemic containment strategies.

The findings from this research are believed to have significant implications for public health policies and strategies aimed at controlling diphtheria.

Acknowledgement

The authours would like to express our sincere gratitude to the constructive feedback provided by the anonymous reviewers and the editorial team, which helped enhance the clarity and rigor of this manuscript.

Conflict of interests

The authors declare that there are no conflicts of interest regarding the publication of this manuscript.

References

Akhi, A.A., Tasnim, F., Akter, S. & Kamrujjaman, M.D. (2023). A mathematical model of diphtheria outbreak in rohingya settlement in bangladesh. *Journal of Mahani Mathematic Research, 122,* 547–563.

Amalia, P.R. & Toaha, S. (2022). Optimal control of mathematical model of diphtheria spreading. DayaMatematis: Jurnal Inovasi Pendidikan Matematik, 10(2), 138–147. https://doi.org/10.26858/jdm.v10i2.35776

Britannica. (2023). "Diphtheria". Encyclopedia Britannica. Retrieved from https://www.britannica.com/science/diphtheria

Centers for Disease Control and Prevention. (2021). Diphtheria. Retrieved from https://www.cdc.gov/diphtheria/index.html

Centers for Disease Control. (2022). Diphtheria. Retrieved from https://www.cdc.gov/diphtheria/about/causes-transmission.html

Coburn, B. J., Wagner, B. G., & Blower, S. (2009). Modeling influenza epidemics and pandemics: insights into the future of swine flu (H1N1). *BMC medicine, 7,* 30. https://doi.org/10.1186/1741-7015-7-30

Delamater, P. L., Street, E. J., Leslie, T. F., Yang, Y. T., & Jacobsen, K. H. (2019). Complexity of the Basic Reproduction Number (R0). *Emerging infectious diseases, 25*(1), 1–4. https://doi.org/10.3201/eid2501.171901

Djaafara, B., Adrian, V., Eriawati, E., Elyazar, I. R.F., Hamers, R.L., Baird, J.K., Thwaites, G.E. & Clapham, H.E. (2020). *Transmission Dynamics and Control Strategies During the 2017 Diphtheria Outbreak in Jakarta, Indonesia: A Modelling Study.*

Egger, M., Razum, O. & Rieder, A. (2017). *Public health kompakt.* De Gruyter, De Gruyter Studium.

Ferguson, N. M., Cummings, D. A., Fraser, C., Cajka, J. C., Cooley, P. C., & Burke, D. S. (2006). Strategies for mitigating an influenza pandemic. *Nature, 442*(7101), 448–452. https://doi.org/10.1038/nature04795

Ghani, M., Utami, I.Q., Triyayuda, F.W., & Afifah, M. (2022). A fractional SEIQR model on diphtheria disease. *Modeling Earth Systems and Environment, 9*, 2199-2219. https://doi.org/10.1007/s40808-022-01615-z

Guerra, F. M., Bolotin, S., Lim, G., Heffernan, J., Deeks, S. L., Li, Y., & Crowcroft, N. S. (2017). The basic reproduction number (R0) of measles: a systematic review. *The Lancet. Infectious*

diseases, 17(12), e420–e428. https://doi.org/10.1016/S1473-3099(17)30307-9

Harris, P. J., & Bodmann, B. E. J. (2022). A mathematical model for simulating the spread of a disease through a country divided into geographical regions with different population densities. *Journal of mathematical biology*, *85*(4), 32. https://doi.org/10.1007/s00285-022-01803-6

Husain, H. S. (2019). An SIR mathematical model for diphtheria disease. *Journal of Physics: Conference Series, 1280*(2). https://doi.org/10.1088/1742-6596/1280/2/022051

Islam, M.D.Z. (2018). *Developing a mathematical model for optimal cost-effectiveness treatment strategies applied to a diphtheria outbreak*. Master's thesis, Department of Mathematics, Bangladesh University of Engineering and Technology and Dhaka-1000.

Izzati, N., Andriani, A. & Robi'aqolbi, R. (2020). Optimal control of diphtheria epidemic model with prevention and treatment. *Journal of Physics: Conference Series, 1663*.

Kanchanarat, S., Chinviriyasit, S., & Chinviriyasit, W. (2022). Mathematical assessment of the impact of the imperfect vaccination on diphtheria transmission dynamics. *Symmetry, 14*(10), 2000. https://doi.org/10.3390/sym14102000

Kucharski, A. J., & Althaus, C. L. (2015). The role of superspreading in Middle East respiratory syndrome coronavirus (MERS-CoV) transmission. *Euro surveillance : bulletin Europeen sur les maladies transmissibles = European communicable disease bulletin*, *20*(25), 14–18. https://doi.org/10.2807/1560-7917.es2015.20.25.21167

Lipsitch, M., Cohen, T., Cooper, B., Robins, J. M., Ma, S., James, L., Gopalakrishna, G., Chew, S. K., Tan, C. C., Samore, M. H., Fisman, D., & Murray, M. (2003). Transmission dynamics and control of severe acute respiratory syndrome. *Science (New York, N.Y.), 300*(5627), 1966–1970. https://doi.org/10.1126/science.1086616

Luo, G., Zhang, X., Zheng, H., & He, D. (2021). Infection fatality ratio and case fatality ratio of COVID-19. *International journal of infectious diseases : IJID : official publication of the International Society for Infectious Diseases, 113,* 43–46. https://doi.org/10.1016/j.ijid.2021.10.004

Milligan, G. & Barrett, A. (2015). *Vaccinology: an essential guide*. Wiley.

National Health Services (NHS) (2022). Diphtheria. Retrieved from https://www.nhs.uk/conditions/diphtheria/

Oli, M., Venkataraman, M., Klein, P., Wendland, L., & Brown, M. (2006). Population dynamics of infectious diseases: A discrete time model. *Ecological Modelling, 198,* 183-194. https://doi.org/10.1016/j.ecolmodel.2006.04.007

Plachouras, D., Sudre, B., Testa, M., Robesyn, E., & Coulombier, D. (2014). Early transmission dynamics of Ebola virus disease (EVD), West Africa, March to August 2014 - Euro surveillance 17 September 2014. *Euro surveillance : bulletin Europeen sur les maladies transmissibles = European communicable disease bulletin*, *19*(37), 20907. https://doi.org/10.2807/1560-7917.es2014.19.37.20907

Rahmi, N., & Pratama, M. (2023). Model Analysis of Diphtheria Disease Transmission with Vaccination, Quarantine, and Hand-Washing Behavior. *JTAM (Jurnal Teori dan Aplikasi Matematika), 7,* 462. https://doi.org/10.31764/jtam.v7i2.13466

Sweileh W. M. (2022). Global research activity on mathematical modeling of transmission and control of 23 selected infectious disease outbreak. *Globalization and health*, *18*(1), 4. https://doi.org/10.1186/s12992-022-00803-x

Thompson, R. N., Stockwin, J. E., van Gaalen, R. D., Polonsky, J. A., Kamvar, Z. N., Demarsh, P. A., Dahlqwist, E., Li, S., Miguel, E., Jombart, T., Lessler, J., Cauchemez, S., & Cori, A. (2019). Improved inference of time-varying reproduction numbers during infectious disease outbreaks. *Epidemics*, *29*, 100356. https://doi.org/10.1016/j.epidem.2019.100356

Truelove, S. A., Keegan, L. T., Moss, W. J., Chaisson, L. H., Macher, E., Azman, A. S., & Lessler, J. (2020). Clinical and Epidemiological Aspects of Diphtheria: A Systematic Review and Pooled Analysis. *Clinical infectious diseases : an official publication of the Infectious Diseases Society of America*, *71*(1), 89–97. https://doi.org/10.1093/cid/ciz808

Wallinga, J., & Teunis, P. (2004). Different epidemic curves for severe acute respiratory syndrome reveal similar impacts of control measures. *American journal of epidemiology*, *160*(6), 509–516. https://doi.org/10.1093/aje/kwh255

Wu, J. T., Leung, K., Bushman, M., Kishore, N., Niehus, R., de Salazar, P. M., Cowling, B. J., Lipsitch, M., & Leung, G. M. (2020). Estimating clinical severity of COVID-19 from the transmission dynamics in Wuhan, China. *Nature medicine*, *26*(4), 506–510. https://doi.org/10.1038/s41591-020-0822-7